

Path Planning for Space Manipulators Exhibiting Nonholonomic Behavior

Evangelos G. Papadopoulos

Department of Mechanical Engineering &
McGill Research Centre for Intelligent Machines, McGill University
3480 University St., Montreal, PQ, Canada H3A 2A7

Abstract

Nonholonomic behavior is observed in free-floating manipulator systems, and is due to the nonintegrability of the angular momentum. Free-floating manipulators exhibit dynamic singularities which cannot be predicted by the kinematic properties of the system and whose location in the workspace is path dependent. Trouble-free Path Independent Workspaces are defined. A joint space planning technique used to control the orientation of the spacecraft by using joint manipulator motions is reviewed, and its limitations are discussed. Finally, a cartesian space planning method that permits the effective use of a system's reachable workspace by planning paths that avoid dynamically singular configurations is proposed and demonstrated by an example.

I. Introduction

Space robotic devices are envisioned to assist in the construction, repair and maintenance of future space stations and satellites. To increase the mobility of such devices, *free-flying* systems in which one or more manipulators are mounted on a thruster-equipped spacecraft, have been proposed [1-4]. To increase a system's life, operation in a *free-floating* mode has been considered [1-6]. In this mode of operation, spacecraft thrusters are turned off, and the spacecraft is permitted to translate and rotate in response to manipulator motions. In practice, this mode of operation can be feasible if the total system momentum is zero; if non zero momentum develops, a system's thrusters must be used to eliminate it.

Free-floating systems exhibit nonholonomic behavior, which is due to the nonintegrability of the angular momentum [5,8]. In addition, in such systems *dynamic singularities* exist, which are functions of the system mass properties and cannot be predicted from its kinematic structure [6,7]. These characteristics complicate the planning and control of such systems. Joint space planning techniques that take advantage of the nonholonomy in such systems were proposed [1,5]. A Self Correcting Planning technique allows the control of a spacecraft's orientation using the manipulator's joint motions [1]. Lyapunov techniques were explored to achieve simultaneous control of a spacecraft's orientation and its manipulator's joint angles, using the manipulator's actuators only. Convergence problems were reported in some cases [5].

In this paper, the fundamental kinematic and dynamic nature of free-floating manipulators is discussed first. The effects of the nonintegrability of the angular momentum and of the dynamic singularities on the behavior of a free-floating system are presented. It is shown that dynamic singularities are *path dependent*, and that a particular workspace point can induce a dynamic singularity or not, depending upon the path taken to reach it. Path Independent Workspaces are defined as regions in which no dynamic singularities occur. The nonholonomic characteristics of free-floating manipulators can be exploited to control the orientation of the spacecraft by closed joint space paths. A joint space planning technique, called Self Correcting Planning, is reviewed, and potential problems in using it are identified. In particular, it is shown that there exist configurations at which a closed path in the joint space will have no effect on the spacecraft orientation. Finally, a Cartesian space path-planning technique which yields paths connecting any two points in the workspace, is presented. This technique avoids dynamically singular configurations, and hence permits the effective use of the full reachable workspace of a free-floating system.

II. Kinematic and Dynamic Modeling of Free-floating Manipulators

The kinematic and dynamic equations needed to model a rigid free-floating manipulator system, see Figure 1, were obtained in [6-8]. A key feature of this modeling is expressing the kinematic and dynamic variables of the system as functions of a set of constant length, body-fixed *barycentric vectors* [8,9]. The dynamics were written using a Lagrangian approach. Here the basic kinematic and dynamic equations are reviewed.

The manipulator joint angles and velocities are represented by the $N \times 1$ column vectors \mathbf{q} and $\dot{\mathbf{q}}$. The spacecraft can translate and rotate in response to manipulator movements. The manipulator is assumed to have revolute joints and an open chain kinematic configuration so that, in a system with an N degree-of-freedom (DOF) manipulator, there will be $6+N$ DOF.

Assuming that no external forces act on the system, the system center of mass (CM) does not accelerate, and the system linear momentum is constant. With the further assumption of zero initial momentum, the system CM remains fixed in inertial space, and can be taken as the origin of a fixed frame of reference.

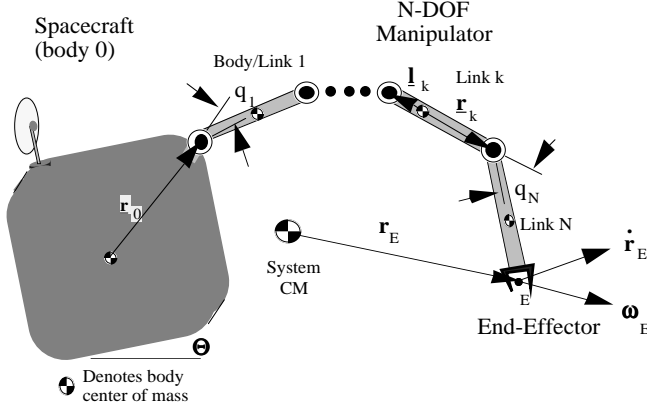


Figure 1. A spatial free-floating manipulator system.

It can be shown that in the absence of external torques, and for zero initial linear momentum, the conservation of momentum equation results in:

$${}^0\omega_0 = -{}^0\mathbf{D}^{-1} {}^0\mathbf{D}_q \dot{\mathbf{q}} \quad (1)$$

where ${}^0\omega_0$ is the spacecraft angular velocity expressed in a frame fixed to it (frame 0), ${}^0\mathbf{D}$ is the 3×3 inertia matrix of the system expressed in the spacecraft frame at the system CM, and ${}^0\mathbf{D}_q$ is a $3 \times N$ mixed inertia matrix. Both ${}^0\mathbf{D}$ and ${}^0\mathbf{D}_q$ are functions of the configuration \mathbf{q} only, and they can be written as functions of the body-fixed barycentric vectors [6-9]. The inverse of ${}^0\mathbf{D}$ always exists because the system inertia matrix is positive definite.

The end-effector inertial linear and angular velocities, $\dot{\mathbf{r}}_E$, and ω_E , are functions of the joint rates $\dot{\mathbf{q}}$ and of the spacecraft angular velocity, ${}^0\omega_0$. Equation (1) can be used to express ${}^0\omega_0$ as a function of $\dot{\mathbf{q}}$, and hence to derive a free-floating system's Jacobian \mathbf{J}^* , defined by:

$$[\dot{\mathbf{r}}_E, \omega_E]^T = \mathbf{J}^* \dot{\mathbf{q}} \quad (2)$$

where \mathbf{J}^* is a function of the orientation Θ of the spacecraft, and given by [6-7]:

$$\mathbf{J}^*(\Theta, \mathbf{q}) = \text{diag}(\mathbf{T}_0(\Theta), \mathbf{T}_0(\Theta)) {}^0\mathbf{J}^*(\mathbf{q}) \quad (3)$$

$\mathbf{T}_0(\Theta)$ is a rotation matrix which describes the orientation of the spacecraft. Due to Eq. (1), \mathbf{J}^* depends not only on the kinematic properties of the system, but also on configuration dependent mass properties, i.e. inertias. Therefore, the singular configurations for a free-floating system, i.e. ones in which ${}^0\mathbf{J}^*$ has rank less than six, are not the same to the ones for fixed based systems, and they depend on the mass distribution.

The equations of motion for a free-floating system can be written in the form [7,8]:

$$\mathbf{H}^*(\mathbf{q}) \dot{\mathbf{q}} + \mathbf{C}^*(\mathbf{q}, \dot{\mathbf{q}}) \dot{\mathbf{q}} = \boldsymbol{\tau} \quad (4)$$

where $\mathbf{H}^*(\mathbf{q})$, is the *reduced* system inertia matrix, $\mathbf{C}^*(\mathbf{q}, \dot{\mathbf{q}})$ contains the nonlinear centrifugal and Coriolis terms. The vector $\boldsymbol{\tau}$ is the torque vector equal to $[\tau_1, \tau_2, \dots, \tau_N]^T$. It is easy to show that the system inertia matrix, \mathbf{H}^* , is an $N \times N$ positive definite symmetric inertia matrix, which depends on \mathbf{q} and the system mass and inertia properties [7,8].

Based on the structural similarity of these equations to the ones derived for a fixed based system, Reference [7] suggested that if singularities of \mathbf{J}^* can be avoided, nearly any control algorithm applied to fixed-based systems can be used in free-floating systems. The nature of free-floating system singularities and workspaces, in conjunction to the nonintegrability of the angular momentum, is addressed next.

III. Characteristics of Free-floating Systems

A. Nonintegrability of the Angular Momentum

The angular momentum, given by Equation (1), cannot be integrated to yield the spacecraft's orientation Θ as a function of the system's configuration, \mathbf{q} , with the exception of a planar two body system [8]. Obviously, this equation can be integrated numerically, but in such case the resulting final spacecraft orientation will be a function of the path taken in the joint space. In other words, different paths in the joint space, with the same initial and final points, will result in different spacecraft orientations. Since the location of the end-effector is also a function of Θ , the same applies to workspace (Cartesian) paths, i.e. moving from one workspace location to another one via different paths results in different final spacecraft orientations. Therefore, closed joint space or workspace paths can change the spacecraft's orientation. This nonintegrability property that introduces nonholonomic characteristics to free-floating systems. However, the nonholonomic behavior results from the particular *dynamic* structure of the system, and is not due to *kinematic* nonintegrable constraints, like the ones experienced by a rolling disk. The use of this nonholonomic behavior to achieve various tasks is described in the following sections.

B. Control in the Joint and Cartesian Space

Assume that one task requires control of the system configuration \mathbf{q} , only. Since \mathbf{H}^* is positive definite, a linearizing feedforward control law $\boldsymbol{\tau} = \mathbf{H}^*(\mathbf{q}) \mathbf{u} + \mathbf{C}^*(\mathbf{q}, \dot{\mathbf{q}}) \dot{\mathbf{q}}$, where $\mathbf{u} \in \mathbf{R}^N$ is an auxiliary control input, reduces the equations of motion to a decoupled second order system, controllable in its joint space.

Assume next that the task is to move the end-effector to some position and orientation, and for simplicity, that $N = 6$. Using Equations (2) and (4), one could design a linearizing and decoupling cartesian space controller, as discussed in [10]. However, such a method would fail at all points where the Jacobian \mathbf{J}^* is singular. Since the rotation matrix \mathbf{T}_0 is not singular, (with the exception of possible representational singularities), then \mathbf{J}^* loses its full rank when:

$$\det[{}^0\mathbf{J}^*(\mathbf{q})] = 0 \quad (5)$$

The above condition shows that singularities in free-floating systems are fixed in joint space. Since ${}^0\mathbf{J}^*$ is a function of configuration dependent inertias, these singularities are different than the ones for fixed base systems, and their location in joint space depend in addition on the dynamic properties of the system; for these reasons, they were called *dynamic singularities* [6].

It is interesting to examine the location of the dynamic singularities in a system's workspace. To do this we need a one to one correspondence from the joint space to the cartesian workspace. However, such a correspondence does not exist, even in the case of a six DOF manipulator, because its end-effector position \mathbf{r}_E , and orientation $\mathbf{T}_{E'}$, are not only functions of the system's configuration \mathbf{q} , but also of the path dependent spacecraft orientation, Θ . Out of all the pairs (Θ, \mathbf{q}) with which a workspace point can be reached, some may correspond to a singular configuration, \mathbf{q}_s . Then a workspace point may or may not induce a dynamic singularity, depending on the joint space path taken to reach it.

To resolve this ambiguity, *Path Dependent Workspaces* (PDW) were defined to contain all workspace locations that may induce a dynamic singularity [6]. To find these points, note that the distance of a workspace location from the system CM, R , does not depend on the spacecraft's orientation, i.e. $R = R(\mathbf{q})$. This equation represents a spherical shell in the workspace. All the singular configurations \mathbf{q}_s are mapped to a set of shells, whose union gives the PDW. If we subtract the PDW from the reachable workspace, we get the *Path Independent Workspace*, (PIW). All points in the PIW are guaranteed not to induce dynamic singularities. Then, any point in the PIW can be reached from all other points in the PIW, by any path that belongs entirely to the PIW.

If the system is in a dynamically singular configuration, the end-effector can move only along directions which lie in a subspace of dimension lower than six; some workspace points are not reachable with small $\delta\mathbf{q}$, whatever $\delta\mathbf{q}$ is. However, it may still be possible to reach any PDW point from any other workspace point, by choosing an appropriate path. This will be demonstrated in Section VI.

IV. Example

Consider the planar free-floating space manipulator shown in Figure 2. The system parameters are given in Table I.

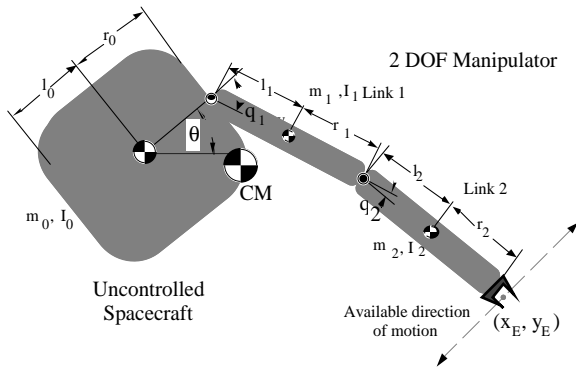


Figure 2. A planar 2 DOF free-floating manipulator, shown in a dynamically singular configuration.

Table I. The system parameters.

Body	l_i (m)	r_i (m)	m_i (Kg)	I_i (Kg m ²)
0	.5	.5	40	6.667
1	.5	.5	4	0.333
2	.5	.5	3	0.250

The zero angular momentum for this system is written using Equation (1) as:

$$\dot{\theta} = D^{-1}\{(D_1+D_2)\dot{q}_1 + D_2\dot{q}_2\} \quad (6)$$

where the inertia scalars D, D_1, D_2 are given by Equations (A1). Multiplying both sides by dt , a nonintegrable Pfaffian equation results, and therefore θ cannot be found as a function of q_1 and q_2 [11]. Nonholonomic behavior is expected.

The system Jacobian for this system is a 2×2 matrix and becomes singular when its determinant is zero [6,8]. The values of q_1 and q_2 which result in dynamically singular configurations can be plotted in joint space as shown in Figure 3. Although the conventional kinematic singularities $q_1 = k\pi, q_2 = k\pi, k=0, \pm 1, \dots$ are included in Figure 3, infinitely more dynamically singular configurations exist which cannot be predicted from the kinematic structure of the manipulator.

Figure 2 shows the system in the singular configuration at $q_1 = -65^\circ, q_2 = -11.41^\circ$, and the spacecraft orientation at $\theta = 40^\circ$. In this configuration, the local inertial motion of the end-effector, starting from rest will be shown in the figure, no matter how the joint actuators are driven. The best a control algorithm can do at such a point is to follow the available direction. All algorithms that use a Jacobian inverse, such as the resolved rate or resolved acceleration control algorithms, fail at such a point. Ones that use a pseudo inverse Jacobian or a Jacobian transpose will likely follow the available direction, but may result in large errors.

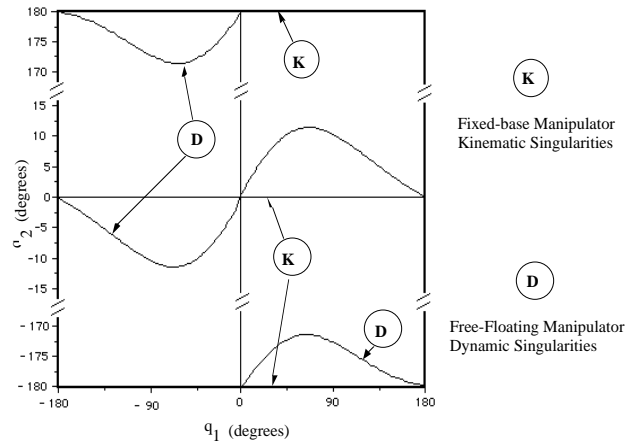


Figure 3. Dynamically singular configurations for the system shown in Figure 2.

Figure 4 depicts the reachable, PDW, and PIW spaces for this example. When the end-effector path has points belonging to the PDW, such as path B in Figure 4, the manipulator may assume a dynamically singular configuration, depending on the path. On the other hand, paths totally within the PIW region, such as path A, can never lead to dynamically singular configurations. In the next section two path planning techniques that take advantage of nonholonomy in free-floating systems are presented.

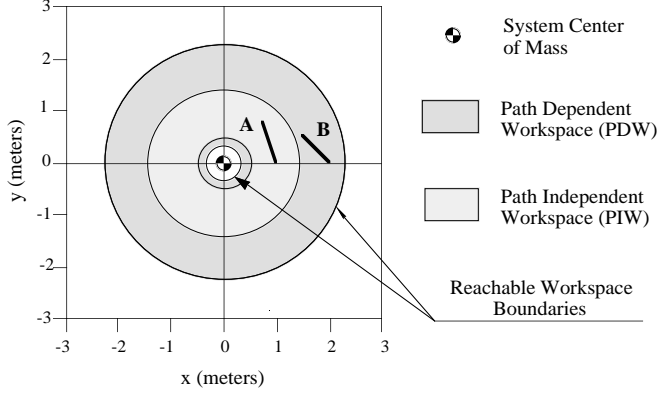


Figure 4. The reachable, Path Dependent, and Path Independent Workspaces, for the system shown in Figure 2.

V. Path Planning in Joint Space

A free-floating system may operate under the Spacecraft-Referenced End-Point Motion Control, in which either the manipulator end-point is commanded to move to a location fixed to its own spacecraft, or a simple joint motion is commanded, such as when the manipulator is to be driven at its stowed position [7]. In general, these motions will change the spacecraft's orientation. However, there are many cases in which this effect may be highly undesirable. For example, the spacecraft may be required to maintain a constant orientation for communication purposes. Therefore, it would be useful to use a special joint path to control a system's orientation, without using limited thruster fuel [1].

Due to the nonholonomic behavior of a free-floating system, a closed path in the manipulator's joint space, will result in a net change in the spacecraft's orientation. Based on this observation, a Self Correcting Planning technique that can correct for deviations from a desired orientation by executing closed joint space paths, has been proposed [1]. Here, this technique is reviewed briefly.

If a spacecraft's orientation is described by the 3-2-1 Euler angles, $\Theta = [\theta_1, \theta_2, \theta_3]^T$, then $\dot{\Theta}$ is written using Equation (1) as [12]:

$$\dot{\Theta} = -S^{-1}(\Theta) \omega_0 = G(\Theta, \mathbf{q}) \dot{\mathbf{q}} \quad (7)$$

where $S^{-1}(\Theta)$ is a nonsingular matrix, except at some isolated points, and $G(\Theta, \mathbf{q}) = -S^{-1}(\Theta) \mathbf{T}_0^0 \mathbf{D}^{-1} \mathbf{D}_q$. For small changes in the configuration \mathbf{q} , Equation (7) is written as:

$$\delta\Theta = G(\Theta, \mathbf{q}) \delta\mathbf{q} \quad (8)$$

where G is a $3 \times N$ matrix. Using a Taylor series expansion of Equation (8), and assuming a joint space closed path along the vectors $\delta\mathbf{V}$, $\delta\mathbf{W}$, $-\delta\mathbf{V}$, $-\delta\mathbf{W}$, the resulting change in the Euler angles $\delta\Theta$ is given by [1]:

$$\delta\theta_i \approx \sum_{l=1}^N \sum_{m=1}^N g_{ilm} \delta V_l \delta W_m \quad (i = 1, 2, 3) \quad (9a)$$

$$g_{ilm} = \sum_{n=1}^3 \left(\frac{\partial G_{im}}{\partial \theta_n} G_{nl} - \frac{\partial G_{il}}{\partial \theta_n} G_{nm} \right) + \frac{\partial G_{im}}{\partial q_l} - \frac{\partial G_{il}}{\partial q_m} \quad (9b)$$

Equation (9) can be used to find the joint space path, as described by vectors $\delta\mathbf{V}$, and $\delta\mathbf{W}$, to achieve a correction in the spacecraft's orientation by $\delta\Theta$. Note that this is possible only if at least one g_{ilm} is non zero.

If the dimension of the manipulator's joint space is three, Equation (9) represents three equations in six unknowns, i.e. δV_i , δW_i , for $i=1,2,3$. The additional constraints:

$$\delta\mathbf{V}^T \delta\mathbf{W} = 0 \quad (10a)$$

$$\delta\mathbf{V}^T \delta\mathbf{V} = \delta\mathbf{W}^T \delta\mathbf{W} \quad (10b)$$

$$\delta V_3 = (\delta V_1 + \delta V_2)/2 \quad (10c)$$

allow complete determination of the required joint space path. This technique assumes that $\delta\Theta$ is small. If a large correction is required, this is broken in smaller ones, and more than one correction cycles are performed. The implementation and the limitation of this method are addressed through the following example.

Example

Consider the system introduced in Section IV. It is desired to estimate the number of joint space closed square paths required to achieve a specified change in the spacecraft's orientation. For this system, and for $\delta\mathbf{V} = [\delta q, 0]^T$, $\delta\mathbf{W} = [0, \delta q]^T$, where δq represents a small change in a joint angle, Equation (9) reduces to:

$$\delta\theta = \left(\frac{\partial G_2}{\partial q_1} - \frac{\partial G_1}{\partial q_2} \right) \delta q^2 = g(q_1, q_2) \delta q^2 \quad (11)$$

where $g(q_1, q_2)$ is a measure of the influence of a closed joint path on a spacecraft's orientation, and given by:

$$g = -2 \frac{d_{01} D_2 \tan(q_1) + d_{12} D_0 \tan(q_2) - d_{02} D_1 \tan(q_1 + q_2)}{D^2} \quad (12)$$

Assuming that at some particular configuration $g(q_1, q_2)$ is non zero, Equation (12) yields the change in orientation of the spacecraft as a function of the area of the closed joint space path. If this path is a square with side δq , the number of paths required to achieve a change $\Delta\theta$ in the orientation, is obtained from Equation (13) as:

$$m \approx \frac{\Delta\theta \ 180^\circ}{(\delta q)^2 \ \pi \ \bar{g}} \quad (13)$$

where both $\Delta\theta$ and δq are in degrees, \bar{g} is the value of $g(q_1, q_2)$ evaluated at $(q_1 + \delta q/2, q_2 + \delta q/2)$, and $\pi = 3.14$.

To demonstrate the use of Equation (13), assume that the system is at $(\theta, q_1, q_2) = (14^\circ, -48^\circ, 145^\circ)$. Then $\bar{g} = g(-43^\circ, 150^\circ) = -0.0495$. If the desired final θ is 10° , then $\Delta\theta = -4^\circ$. Assuming a square joint path of side $\delta q = 10^\circ$, and using Equation (13), we find that the required number of square paths is $m = 46$. Figure 5 shows the orientation as a function of m . After the execution of 46 closed joint paths, the spacecraft's orientation becomes 10.06° .

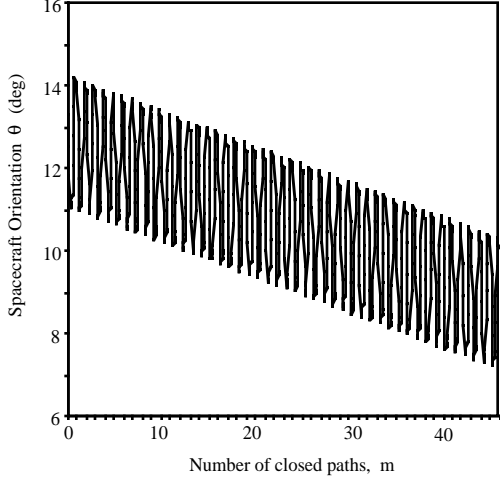


Figure 5. Changes in the spacecraft orientation q , during the execution of closed joint space paths.

As discussed earlier, this technique can be used if \bar{g} is non zero. However, \bar{g} becomes zero for certain configurations \mathbf{q} , shown in Figure 6. Note the similarity with Figure 3. When the system manipulator is in one of these configurations, its spacecraft orientation *cannot* be affected by small joint space closed paths.

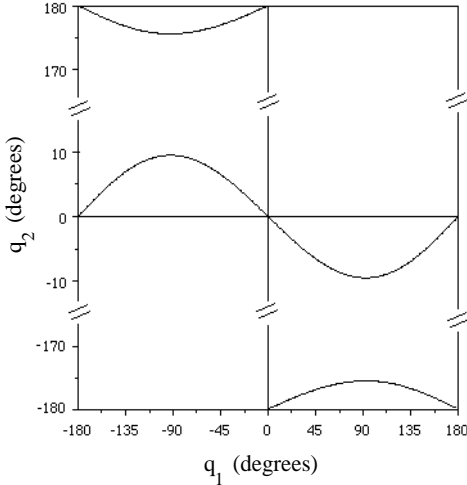


Figure 6. Configurations at which joint motions have no effect on the spacecraft's orientation q .

In addition, a workspace location may have this property or not depending on the path taken to reach it. These configurations can be mapped to cartesian space areas, using $\mathbf{R} = \mathbf{R}(\mathbf{q})$ as discussed in Section III B. For this example, one can show that \mathbf{g} is non zero everywhere in the system's PIW. In other words, if the end-effector is in the PIW, the spacecraft orientation is always affected by closed joint space paths. However, when the end-effector is in the PDW, closed joint paths may not result in changes in the orientation, and hence this is limiting the extent to which this method can be used.

VI. Path-planning in the Cartesian Workspace

The previous techniques can be used to find joint paths that either correct a spacecraft's orientation during a manipulator's motion, or simultaneously control the spacecraft orientation, and the manipulator's configuration; they don't deal with Cartesian space path planning. However, in many important applications, the system will operate under an Inertially-Referenced End-Point Motion Control mode [7]. Here, the primary task is to move the end-effector of the manipulator, from one inertial location to another. As discussed in Section IV, if the path has segments in the PDW, dynamic singularities may occur. This problem becomes even more serious when the end-effector carries a load, because in such a case, the PIW is severely reduced [8]. To avoid these problems, either the workspace should be restricted to the PIW, or a planning technique that can avoid dynamic singularities should be employed. In this section, one such technique is developed.

Assume that the task is to move the end-effector from point A to point D, without encountering dynamic singularities that will prevent reaching the destination point. Then, the following strategy can be used:

(a) Start from the final desired spacecraft orientation and end-effector position/orientation, and move under joint space control to some point C of the PIW. Such a motion is not subject to the effects of dynamic singularities, because these affect the cartesian motion, only. Record the path taken. The system reaches point C with \mathbf{q}_{DC} and Θ_{DC} .

(b) Start from the initial desired spacecraft orientation and end-effector position/orientation, and move under joint space control to some point B of the PIW. The system reaches point C with \mathbf{q}_{AB} and Θ_{AB} . Note that other points B or C located outside the PIW can be used also, if they are reachable from A, and D at configurations "sufficiently" away from singular ones. Such points can be useful in the event that the PIW is zero. However, more research is needed in this case.

(c) Move from point B to point C, using any path. The system reaches point C with \mathbf{q}_{AC} and Θ_{AC} . In general, these are different than \mathbf{q}_{DC} and Θ_{DC} .

(d) Using small cyclical motions of the end-effector, change the spacecraft orientation from Θ_{AC} to Θ_{DC} . The configuration changes from \mathbf{q}_{AC} to \mathbf{q}_{DC} , since the end-effector does move around the same point in cartesian space. This is in contrast to the technique in Section V, where the configuration \mathbf{q} remains constant after one cycle.

(e) Use the recorded path during step (a), to move to point D.

The fact that small cyclical motions in the cartesian space can change a spacecraft's orientation is due to the following equation, obtained by combining Equations (2) and (7), and using an Euler angle representation for the end-effector orientation:

$$\delta\Theta = \mathbf{G}(\Theta, \mathbf{q}) \{ \text{diag}(\mathbf{I}, \mathbf{S}^{-1}(\Theta_E)) \mathbf{J}^* \}^{-1} \delta\mathbf{x}_E = \mathbf{G}^*(\Theta, \mathbf{x}_E) \delta\mathbf{x}_E \quad (14)$$

where $\delta\mathbf{x}_E = \delta[\mathbf{r}_E, \Theta_E]^T$ is a small change in the end-effector position/orientation. The 3×6 matrix \mathbf{G}^* is written as a function of Θ , and \mathbf{x}_E , because if these are given, and if $N=6$,

then \mathbf{q} can be found uniquely. Note that Equation (14) has the same structure to Equation (8), though more complicated. Since \mathbf{J}^* is invertible in the PIW, \mathbf{G}^* exists and hence, closed paths in the cartesian space will result in changes in the orientation of a system's spacecraft. This technique is illustrated below by an example.

Example

Consider again the example system introduced in Section IV. The end-effector is initially at point A: $(x,y) = (2,0)$, which belongs in the system's PDW, see Figure 7. The initial configuration of the system is $(q_1, q_2) = (-58^\circ, 60.3^\circ)$ which corresponds to an initial spacecraft orientation $\theta = 21^\circ$. Assume that the end-effector is commanded to reach point D: $(x,y) = (1.5,1.5)$. As the end-effector moves on a straight line from the initial to the desired location, a dynamic singularity occurs at point E, where $(\theta, q_1, q_2) = (-32.4^\circ, 74.24^\circ, 10.6^\circ)$, see Figure 7.

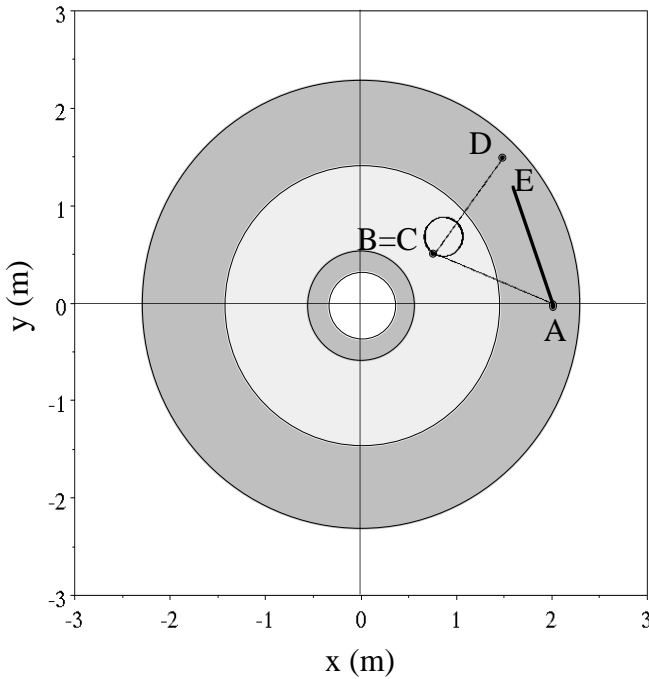


Figure 7. A Dynamic Singularity at point E does not allow the end-effector to move from point A to D. Path ABCD avoids singularities by employing small circles at point B.

The end-effector stops at this point if an inverse Jacobian planning or control algorithm is used, or deviates from the desired final point if a transposed Jacobian control algorithm is used [7,8].

Next, the algorithm introduced above is applied. The task is to reach point D, with $\theta \approx 3^\circ$. This θ corresponds to $(q_1, q_2) = (39.4^\circ, 22.2^\circ)$. First, the end-effector is moved from the desired point D, to some PIW point C: $(0.8, 0.5)$, see path DC in Figure 7. Here a straight line motion is used, and C is reached with $\theta_{DC}=49.1^\circ$. Next, the end-effector is moved from the initial point A, to point B, which for simplicity is taken equal to point C. The end-effector reaches point B: $(0.8, 0.5)$ with $(\theta, q_1, q_2) = (14.5^\circ, -49.4^\circ, 145.9^\circ)$.

The next task is to change the orientation of the spacecraft, from $\theta_{AC}=14.5^\circ$, to $\theta_{DC}=49.1^\circ$. To this end, the end-effector is commanded to follow 11 circular paths, with radius .2m, as shown in Figure 7.

The required number of circles has been found by trial and error. After the execution of these circles, the orientation θ changes to 48.9° . Next, the end-effector is moved to D, following the prerecorded path DC in the opposite direction, and reaches D with $(\theta, q_1, q_2) = (3.3^\circ, 38.9^\circ, 22.7^\circ)$. Note that not only the destination point D, but also the desired final spacecraft orientation has been reached. If a closer match in orientation is required, a smaller circle radius and more circles should be employed. Figure 8 depicts the change of θ during as a function of the length of the total path ABCD.

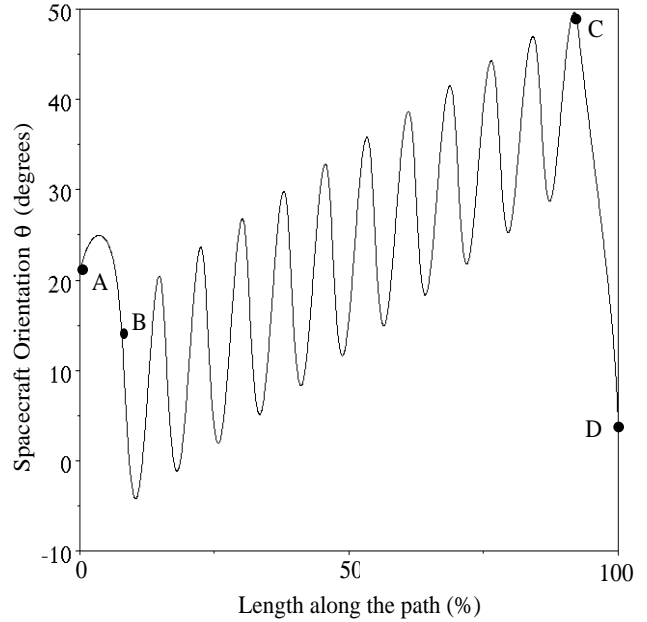


Figure 8. The orientation of the spacecraft q as a function of the path ABCD, shown in Figure 6.

VII. Conclusions

In this paper the nonholonomic behavior of free-floating manipulators is addressed and attributed to the nonintegrability of the angular momentum. It is shown that free-floating manipulators exhibit dynamic singularities which cannot be predicted by the kinematic properties of the system and whose location in the workspace is path dependent. Trouble-free Path Independent Workspaces are defined. A joint space planning technique that uses manipulator joint motions to control a spacecraft's orientation was reviewed. It was shown that in some system configurations, joint manipulator motions cannot affect a spacecraft's orientation, and hence, such a technique must be used with caution. Finally, a Cartesian space planning method was presented that permits the effective use of a system's reachable workspace by planning paths which avoid dynamically singular configurations.

VIII. Acknowledgments

The support of this work by the Natural Sciences and Engineering Council of Canada (NSERC) is gratefully acknowledged.

References

- [1] Vafa, Z., and Dubowsky, S., "On the Dynamics of Space Manipulators Using the Virtual Manipulator, with Applications to Path Planning," *J. Astr. Sciences*, Vol. 38, No. 4, October-December 1990, pp. 441-472.
- [2] Alexander, H., and Cannon, R., "Experiments on the Control of a Satellite Manipulator," *Proc. 1987 American Control Conf.*, Seattle, WA, June 1987.
- [3] Umetani, Y., and Yoshida, K., "Experimental Study on Two Dimensional Free-Flying Robot Satellite Model," *Proc. NASA Conf. on Space Telerobotics*, Pasadena, CA, January 1989.
- [4] Masutani, Y., Miyazaki, F., and Arimoto, S., "Sensory Feedback Control for Space Manipulators," *Proc. IEEE Int. Conf. on Robotics & Automation*, Scottsdale, AZ, May 1989.
- [5] Nakamura, Y., and Mukherjee, R., "Nonholonomic Path Planning of Space Robots via Bi-directional Approach," *Proc. IEEE Int. Conf. on Robotics & Automation*, Cincinnati, OH, May 1990.
- [6] Papadopoulos, E., and Dubowsky, D., "On the Dynamic Singularities in the Control of Free-Floating Space Manipulators," *Proc. ASME WAM*, San Francisco, ASME DSC-Vol. 15, Dec. 1989.
- [7] Papadopoulos, E., and Dubowsky, S., "On the Nature of Control Algorithms for Free-floating Space Manipulators," *IEEE Trans. on Robotics and Automation*, Vol. 7, No. 6, Dec. 1991, pp. 750-758.
- [8] Papadopoulos, E., "On the Dynamics and Control of Space Manipulators," Ph.D. Thesis, Department of Mechanical Engineering, MIT, October 1990.
- [9] Wittenburg, J., *Dynamics of Rigid Bodies*, B.G. Teubner, Stuttgart, 1977.
- [10] Khatib, O., "A Unified Approach for Motion and Force Control of Robot Manipulators: The Operational Space Formulation," *IEEE J. of Robotics and Automation*, Vol. RA-3, No. 1, Feb. 1987, pp. 43-53.
- [11] Korn, G., and Korn, T., *Mathematical Handbook for Scientists and Engineers*, Second Edition, McGraw-Hill, New York, NY, 1968.
- [12] Hughes, P., *Spacecraft Orientation Dynamics*, John Wiley, New York, NY, 1986.

Appendix A

The inertia terms used in the example are, see also [7]:

$$D_j = \sum_{i=0}^2 d_{ij}, \quad {}^0\mathbf{D} \equiv \mathbf{D} = \sum_{i=0}^2 D_j, \quad {}^0\mathbf{D}_q = [D_1 + D_2 \quad D_2] \quad (\text{A1})$$

where the d_{ij} terms are given by:

$$\begin{aligned} d_{00} &= I_0 + \frac{m_0(m_1+m_2)}{M} r_0^2 \\ d_{10} &= \frac{m_0 r_0}{M} \{ l_1(m_1+m_2) + r_1 m_2 \} \cos(q_1) = d_{01} \\ d_{20} &= \frac{m_0 m_2}{M} r_0 l_2 \cos(q_1+q_2) = d_{02} \\ d_{11} &= I_1 + \frac{m_0 m_1}{M} l_1^2 + \frac{m_1 m_2}{M} r_1^2 + \frac{m_0 m_2}{M} (l_1+r_1)^2 \\ d_{21} &= \left\{ \frac{m_1 m_2}{M} r_1 l_2 + \frac{m_0 m_2}{M} l_2 (l_1+r_1) \right\} \cos(q_2) = d_{12} \\ d_{22} &= I_2 + \frac{m_2(m_0+m_1)}{M} l_2^2 \end{aligned} \quad (\text{A2})$$

The lengths l_i, r_i ($i=0,1,2$) are defined in Figure 2. M is the total system mass, $M = m_0 + m_1 + m_2$.